Gaussian Beams in the Optics Course

Enrique J. Galvez

Department of Physics and Astronomy,

Colgate University, Hamilton, NY 13346

(Dated: January 24, 2006)

Abstract

We introduce the physics of high-order Gaussian beams to the treatment of Gaussian beams in the undergraduate optics course. Of particular interest are Laguerre-Gauss beams, which provide the basis for discussing the new and increasingly important concept of the orbital angular momentum of light. We also describe laboratory exercises that complement the class material.

I. INTRODUCTION

Optics is a popular choice as an upper-level elective course in the undergraduate physics curriculum. It is a topic with many interesting phenomena and applications. The solutions of problems are often elegant and at a mathematical level that undergraduates can easily grasp. Since optics is the basis of many scientific and technological applications, students leave the course with a solid understanding of optics fundamentals and with a useful set of laboratory skills.

The standard optics course contains several core topics: light waves, geometric optics, polarization, interference and diffraction. It is up to the instructor to decide what other topics to include (e.g., Fourier optics, holography, coherence, lasers, nonlinear optics and quantum optics, to name a few). However, optics has evolved tremendously in the last few decades. New subfields and technologies have appeared in response to major discoveries. Therefore, it is important to re-evaluate the evolution of the core material and the selection of specialty topics.

The advent of the laser has had a huge impact in optics. It has led to technological applications in most fields of science and engineering. The teaching laboratories of the optics course have been significantly enhanced with the use of lasers. Yet laser fundamentals and laser-beam propagation do not receive prominent roles in most optics textbooks. The topic of Gaussian beams traditionally describes the characteristics of laser beams and their propagation. It is important for finding useful parameters of the light beam and its propagation through an optical system.

In the last decade we have seen the emergence of an extension of Gaussian beams: high-order Gaussian modes. These are high-order solutions of the paraxial wave equation. High-order Gaussian modes of light are a hidden treasure. They are rich with physics and wave phenomena. The most interesting families of Gaussian beams are the Laguerre-Gauss beams, which are the solutions to the wave equation in cylindrical coordinates. They bring a new fundamental concept to optics: orbital angular momentum. This is the angular momentum of the light that arises when the beam has a helical wave-front.[1] These types of beams also serve as an introduction to an interesting new field in optics: singular optics.[2,3]

In this article we present the framework for covering Gaussian beams to include the discussion of high-order beams and orbital angular momentum. This treatment reflects

our own efforts and experience at incorporating high-order Gaussian beams into our optics course at Colgate University. In Sec. II we describe how to introduce the fundamental zero-order solution of the paraxial wave equation. We continue in Sec. III with a discussion of the high-order solutions of the wave equation in rectangular coordinates: Hermite-Gauss beams. The solution of the wave equation in cylindrical coordinates, giving rise to Laguerre-Gauss beams, is presented in Sec. IV. Section V presents a discussion of the new form of angular momentum carried by Laguerre-Gauss beams. In all sections we present laboratory experiments that can be used to complement the class material.

II. ZERO-ORDER GAUSSIAN SOLUTION

Optics courses often start with a review of waves and the wave equation (see for example Ref. 4). This begins with a discussion of light waves propagating in one dimension. The wave has a phase given by $(kz-\omega t)$ when propagating along the z direction, where $k = 2\pi/\lambda$ is the wave number, ω is the angular frequency, and λ is the wavelength. The discussion evolves into a treatment of waves propagating in three dimensions. Two types of three-dimensional waves are particularly useful: plane waves and spherical waves. A plane wave is in essence a one-dimensional wave propagating in an arbitrary direction, with a phase given by $(\mathbf{k}\cdot\mathbf{r}-\omega t)$, where $\mathbf{k}$ is the propagation vector and $\mathbf{r}$ is the position. A spherical wave propagates symmetrically from the origin. It has a phase given by $(kr-\omega t)$ and an amplitude proportional to $1/r$, where $r = |\mathbf{r}|$.

A laser beam is a narrow collimated beam of light that diverges slowly as it propagates. The wave function that describes it is a solution of the paraxial wave equation. We found it useful to begin the discussion of Gaussian beams by first estimating the main terms in the solution.[5] This is a healthy exercise because it invokes intuition and helps students understand the exact form of the solution. Gaussian beams must be represented by a wave function that propagates mainly in one dimension and very slowly in the other two dimensions. Thus, the wave function has the characteristics of both plane and spherical waves. The two important components of a wave function are its amplitude and phase. Let us assume that the main axis of the light beam is aligned along the z direction. Because of the small but finite expansion of the beam, its amplitude must decrease with z. Since the amplitude is restricted to small values of x and y, then it must fall rapidly as x or y

increase. The Gaussian shape specified by $\exp[-(x^2+y^2)/w^2]$, where w is the width of the beam, seems intuitively appropriate. Because of the mostly one-dimensional propagation the main phase term should be of the form $(kz-\omega t)$ for points along the axis, but because of the expansion of the beam, its wave-front, the surface containing points of equal phase, it must be spherical. Therefore, the phase must also contain a term that resembles a spherical wave for finite values of x and y.

After this step one then proceeds with a more formal method of solving the wave equation. The solution is set up to have the form

$$\Psi(x,y,x,t) = \mathcal{E}(x,y,z)e^{i(kz-\omega t)}. \tag{1}$$

The steps that follow consist of deriving the Helmholtz equation and making the approximations applicable to Gaussian beams. The derivation leads to the paraxial wave equation:

$$\frac{\partial^2\mathcal{E}}{\partial x^2} + \frac{\partial^2\mathcal{E}}{\partial y^2} + 2ik\frac{\partial\mathcal{E}}{\partial z} = 0. \tag{2}$$

To obtain the zero-order solution of Eq. 2 we first introduce a trial solution of the form

$$\mathcal{E}_0(x,y,z) = Ae^{ik(x^2+y^2)/[2q(z)]}e^{ip(z)}. \tag{3}$$

The solution of Eq. 3 then reduces to finding $q(z)$ and $p(z)$. The trial solution of Eq. 3 fixes the dependence on the transverse coordinates x and y, forcing the solution to have a symmetric transverse profile. A complex solution for q will lead to the terms introduced intuitively above. The final solution is[5]

$$\mathcal{E}_0(x,y,z) = \frac{A}{w(z)}e^{-(x^2+y^2)/w(z)^2}e^{ik(x^2+y^2)/[2R(z)]}e^{i\phi(z)}. \tag{4}$$

The width of the beam or spot size is given by

$$w(z) = w_0\sqrt{1+\frac{z^2}{z_R^2}}, \tag{5}$$

where w_0 is the waist of the beam and $z_R = \pi w_0^2/\lambda$ is the Rayleigh range. This solution agrees with the terms obtained intuitively before. It contains an amplitude that decreases axially with z via $w(z)$, and transversely it falls as a function of x and y via the Gaussian term.

It is important to follow this solution with a discussion of Gaussian beam propagation and the effect of lenses on Gaussian beams of various widths and wave-front radii $R(z)$.

This formalism predicts the *correct* size and location of the beam waist.[5,6] The discussion of Gaussian-beam propagation can be either short, using Ref. 5 as a basis, or expanded by introducing the elegant "ABCD" matrix formalism.[7]

The treatment of Gaussian beams also brings to the forefront a discrepancy between the predictions of wave optics and those of ray optics: the finite waist w_0 of the beam. Geometric optics, which uses ray-optics for describing imaging with lenses, predicts a zero waist at the focal point of a lens when a collimated beam is incident on the lens. It is wave optics that gives the correct beam width at the focal point. Ignoring a discussion of Gaussian beams leads to misconceptions, and can give the wrong results in the laboratory.[6] Usually the instructor can remedy this deficiency when discussing diffraction and resolution, but this seems unnecessarily qualitative when the exact solution is at hand. In addition, the discussion on the waist of the Gaussian beam can be used to reinforce the concept of resolution in the chapter on diffraction.

A useful laboratory exercise on this subject is to challenge students to send a laser beam through a small pinhole. We give the students a laser, an assortment of lenses, a pinhole (e.g., 50 μm in diameter), and a detector. The exercise is conceived in such a way that in order to complete the experiment students have to expand the beam. Successful execution of the experiment also necessitates a measurement of the divergence of the laser beam; this could be an exercise that is assigned before the challenge.

The phase given by $k(x^2 + y^2)/[2R(z)]$ in Eq. 4 accounts for the spherical wave-front of the beam. The radius of curvature of the wave-front, given by $R(z) = z + z_R^2/z$, has a dependence on z that is interesting in itself. The Gouy phase, given by $\phi(z) = \tan^{-1}(z/z_R)$, is also interesting. It is a consequence the propagation of the Gaussian beam, and changes most rapidly when the beam goes through a focal point.

The phase of the wave is measured by interference. Thus, the properties of Gaussian beams can be revisited later in the course when covering the chapter on interference.

A convenient optical setup to study wave-fronts is a Mach-Zehnder interferometer,[8] shown in Fig. 1. The setup and alignment of the Mach-Zehnder interferometer is a lab exercise in itself. This alignment job can be quite straight forward if done systematically with an iris aligned with the holes of an optical breadboard. This method is described in detail in the Appendix. We find non-polarizing cube beam splitters convenient for use in interferometers. They are reasonable in cost compared to other optical components (e.g., a beam splitter

of 1-cm in size, such as Melles Griot part number 03BSC003, costs about $150). It is also good practice to use laser beams polarized along the vertical or horizontal directions. If the input polarization is oriented at an arbitrary angle, differences in the reflection coefficients of the beam splitters and mirrors may produce changes in the state of polarization that depend on the interferometer path taken by the light, and thus reducing the visibility of the interference pattern.

When the beams coming from both arms of the interferometer are not exactly collinear the interference pattern consists of straight fringes, as shown in Fig. 2a. These can either be projected onto a screen with a diverging lens placed after the interferometer, or sent to a CCD camera without a lens. By inserting a diverging lens in one of the arms we can investigate the spherical wave-front of the beam: the interference of collinear beams with different radii of curvature produces the "bulls-eye" pattern shown in the Fig. 2b.

One can also use the interferometer to observe the Gouy phase. This is done by placing a converging lens in one of the arms of the interferometer such that it focuses the beam going through that arm outside the inteferometer. A CCD camera placed in the path of the beams will show a bulls-eye interference pattern produced by the focused beam and the unfocused beam coming from the other arm of the interferometer. By moving the camera along the propagation axis of the beams about the beam waist one can see the fringes shifting due to the Gouy phase. Note that this is done *without* changing the path-length difference of the light in the interferometer

We can make the interferometer very stable against vibrations by using "pedestal" mounts, and by making the dimensions of the interferometer as small as possible. By mounting one of the mirrors on a translation stage and putting a piezo-electric ceramic as a spacer in the stage, one can scan the interference fringes by applying a voltage to the piezo-electric (e.g., the piezo-electric from Thorlabs model AE0505D8 costs about $130). The 0-to-150-volt driver of the piezo-electric is a low-cost high-voltage amplifier (e.g., EMCO High Voltage part number Q02-24 costs about $80). An inexpensive way to scan the fringes is to attach a rubber band to the back of one of the mirror mounts and then to pull the other end of the rubber band in a systematic way.

III. HIGH-ORDER HERMITE-GAUSS SOLUTIONS

The high-order solutions of the paraxial wave equation depend on the system of coordinates that we use. It is natural to start the discussion with the solution in rectangular coordinates. Rectangular solutions of the wave equation also have a familiar mathematical formalism for the students.

We start by revisiting the paraxial wave equation (Eq. 2), and introducing the more general trial solution:

$$\mathcal{E}(x,y,z) = Ag(x,z)h(y,z)e^{ik(x^2+y^2)/[2q(z)]}e^{ip(z)}. \tag{6}$$

Note that now we allow the solution to have independent x and y dependencies. Substituting Eq. 6 into Eq. 2 yields[5,7,9] two Hermite differential equations for g and h. The final solution is

$$\mathcal{E}_{m,n}(x,y,z) = \frac{A}{w(z)}H_m(\frac{\sqrt{2}x}{w(z)})H_n(\frac{\sqrt{2}y}{w(z)})e^{-(x^2+y^2)/w(z)^2}e^{ik(x^2+y^2)/[2R(z)]}e^{i\phi(z)}. \tag{7}$$

A beam described by this solution is known as a Hermite-Gauss beam. The indices m and n of the Hermite polynomials H_m and H_n label particular solutions or modes. We define the order of the solution by $N = n + m$. Modes of the same order are degenerate in laser resonators. Since $H_0 = 1$, the solution of Eq. 4 for $n = m = 0$ is the zero-order solution described in the previous section. Aside from the Hermite polynomials, the other terms of Eq. 7 are the same as those of Eq. 4 except for the Gouy phase, which is given by a modified expression: $\phi(z) = (N+1)\tan^{-1}(z/z_R)$. The dependence of the Gouy phase on the order N gives rise to the higher resonant frequencies of (high-order) transverse modes in laser resonators. The constant term that normalizes the total intensity is given by[10] $A = [2^{1-N}/(\pi n!m!)]^{1/2}$.

The Hermite-Gauss solutions have a variety of interesting shapes and forms that can be investigated in the laboratory by use of an open-frame laser with a thin wire placed in the cavity.[10,11] Losses by scattering off the wire cause the laser to oscillate in a mode that has its nodes along the wire. An alternative method is to use a thin coverslip as an etalon and frequency select the mode by tilting the etalon.[12] By sending the beam through an interferometer one can examine the π phase difference between adjacent lobes, as described below.

A convenient way to produce high-order modes is to use computer-generated holograms.

Binary amplitude holograms are simple to make, but require a technology that is increasingly becoming obsolete: black-and-white film photography. This method consists of taking a photograph of a computer printout of the pattern. The image on the film (i.e., the negative) is the grating. If the pattern of the grating is composed of two staggered gratings, then the first-order diffracted beams will closely resemble the $N = 1$ Hermite-Gauss beam, as shown in the bottom pane of Fig. 3a.

By using the grating in one of the arms of the interferometer (G in Fig. 1) one can interfere a beam in a high-order mode with the original beam in the zero-order mode. The interference pattern produces a staggered set of fringes, as shown in Fig. 2c. The experiment also demonstrates the principle of holography: the interference pattern is a reconstruction of the staggered grating (i.e., the hologram). A low-cost solution for making the grating is to reduce the computer printout of Fig. 3a with a photocopy machine to about 6 mm in size, and make the last photocopy onto transparency paper.

IV. HIGH-ORDER LAGUERRE-GAUSS SOLUTIONS

The physics of high-order modes gets much more interesting when we consider the solutions of the paraxial equation in cylindrical coordinates. This solution is not easily found in the literature,[13] but perhaps it is too mathematical to cover it in an undergraduate optics course. The solution in cylindrical coordinates ($\rho = \sqrt{x^2+y^2}, \theta = \tan^{-1}(y/x), z$) is given by

$$\mathcal{E}_{p,\ell}(\rho,\theta,z) = \frac{A}{w(z)}\left(\frac{\sqrt{2}\rho}{w(z)}\right)^{\ell} L_p^{\ell}\left(\frac{2\rho^2}{w(z)^2}\right) e^{-\rho^2/w(z)^2} e^{ik\rho^2/[2R(z)]} e^{i\ell\theta} e^{i\phi(z)}. \tag{8}$$

The solutions contain the associated Laguerre function L_p^{ℓ}, and therefore called Laguerre-Gauss modes. The subindices p and ℓ label the solutions of order $N = 2p + |\ell|$, which also reduce to the zero-order solution when $p = \ell = 0$. The normalization constant is given by[10] $A = p!\{2/[\pi p![(|\ell| + p)!)]\}^{1/2}$.

One of the characteristics of the solution is that the amplitude has a purely radial dependence. When $\ell \neq 0$ and $p = 0$ the beams have a characteristic single-ringed "doughnut" shape, with the radius of the doughnut given by $w\sqrt{\ell/2}$. The radius of curvature of the wave-front and the Gouy phase are the same as in the high-order rectangular solutions.

The most interesting term is the one containing the phase $\ell\theta$. Ignoring for the moment the correction due to the radius of curvature of the phase front and the Gouy phase (or

equivalently assuming $R(z) \to \infty$), the phase of the wave is given by

$$\psi(\rho, \theta, z) = kz + \ell\theta. \tag{9}$$

Points of constant phase (i.e., the wave-front) form a helix of pitch λ, as shown in Fig. 4 for the case $\ell = 1$. For $\ell > 1$ the wave-front consists of ℓ intertwined helices. In a given transverse plane the phase depends on θ. At $\rho = 0$ the phase is undefined. At that point there is a phase singularity or vortex,[14] and the amplitude of the wave is zero.

These beams are easily produced with a forked diffraction grating.[15] Figure 3b shows a charge-1 forked diffraction grating. The pattern shown is a graph of the binary valued interference pattern of a Laguerre-Gauss beam with $\ell = 1$ and a non-collinear plane wave. If the propagation vectors of the wave of order ℓ and a plane wave of order zero are $(0, 0, k)$ and $(k \sin\beta, 0, k \cos\beta)$, respectively, then the phase difference between them at the $z = 0$ plane is

$$\psi(x, y, 0) = \ell \tan^{-1}(y/x) - xk \sin\beta. \tag{10}$$

The binary forked grating of charge $q = \ell$ is the filled contour graph of the function

$$f(x, y) = \begin{cases} 1 & 2m\pi + \epsilon\pi/2 \leq \psi(x, y, 0) < (2m + 1)\pi - \epsilon\pi/2 \\ 0 & (2m + 1)\pi - \epsilon\pi/2 \leq \psi(x, y, 0) < (2m + 2)\pi + \epsilon\pi/2, \end{cases} \tag{11}$$

where m is an integer. One can set a graphing routine to fill with white where $f(x, y) = 1$, and black where $f(x, y) = 0$. The ratio of the white to black thickness is given by $(1 - \epsilon)/(1 + \epsilon)$. The pattern of Fig. 3b was made with $\epsilon = 0.11$.

One can use the interference setup of Fig. 1 to investigate the peculiar phase of Laguerre-Gauss beams. Similar to the discussion in the previous section, we place a charge-1 forked diffraction grating in one of the arms of the interferometer. In general, when a zero-order input beam is incident on a grating of charge q, the n-th diffracted order is a Laguerre-Gauss beam with $\ell = qn$ (see also Ref. 16). In the arm with the $q = 1$ forked grating we steer the first order (i.e., with $\ell = 1$) to interfere with the zero order mode going through the other arm. When the reference beam is unexpanded and non collinear, the interference pattern is a recreation of the forked hologram, as shown in Fig. 2e. When the unexpanded reference beam is collinear with the one in the Laguerre-Gauss mode, the interference pattern consists of an off-axis "blob" that gyrates about the central spot when the path difference between

the two interferometer arms is varied (see for example Ref 17). If the reference beam is expanded, then the interference pattern has a unique spiral shape, as shown in Fig. 2f.

There are other interesting aspects of high-order modes of Gaussian beams that can be studied in upper-level undergraduate laboratory projects. One is the conversion between Hermite-Gauss and Laguerre-Gauss modes using astigmatic mode converters,[10,11,18] which also constitutes an important application of the Gouy phase. Other interesting solutions to the wave equation are the "diffraction-free" Bessel beams[19] and the solution of the wave equation in elliptical-cylindrical coordinates, which is expressed in terms of Mathiew functions.[20]

V. ORBITAL ANGULAR MOMENTUM

As mentioned before, Laguerre-Gauss beams carry orbital angular momentum. This is different from spin angular momentum, which is associated with the circular polarization of the light. Orbital angular momentum has been discussed extensively in the literature.[21,22] It can be understood intuitively by analyzing the wave-front of Fig. 4. In free space the local momentum of the beam is normal to the surface of the wave-front. Since this momentum has an azimuthal component, then there is a finite longitudinal component of the angular momentum. A rigorous derivation shows that the total angular momentum of the beam along the propagation direction is proportional to ℓ.[18,21,22]

There have been numerous demonstrations of the transfer of orbital angular momentum to matter. All of the demonstrations involve optical tweezers. Microscopic objects (e.g., micron-sized latex spheres) can be trapped in the high-intensity region of the doughnut and carried along the ring by the tilted wave-front.[23] In this case one can think that the wave-front is doing the same job that a rotating drill bit does to the filings after shaving them off the drilled material. It is important to note that the light is *not* traveling in a helical trajectory. The helical surface is the mathematical locus of points of equal phase. Absorptive particles have been shown to rotate by the transfer of angular momentum,[24] and larger irregular objects have been set to rotate via light-induced torques.[25] Unfortunately these experiments are not easy to reproduce because of the low efficiency in producing Laguerre-Gauss beams with the forked amplitude gratings. The recent report of a low-cost phase plate[26] holds promise for implementing a feasible angular momentum transfer

demonstration in the undergraduate laboratory.

The orbital angular momentum carries over to the photon level when the photons are propagating in that mode of the light. This is an interesting but challenging concept to grasp. We must imagine that a single photon has a spatial extension in the transverse direction in order to carry the phase properties of a Laguerre-Gauss mode, and thus orbital angular momentum. The total angular momentum of a photon can be expressed as[18,22]

$$L = \sigma\hbar + \ell\hbar, \tag{12}$$

where $\sigma = \pm 1$ represents the spin angular momentum of the photon.

VI. CONCLUSIONS

The topic of Gaussian beams provides students with the fundamentals for understanding the physics of laser beams and their propagation. Given the wide-spread use of lasers today, this material should be an essential part of a course on optics. The coverage of high-order Gaussian modes serves to deepen the discussion of light waves, and to underscore the key components of the wave function: amplitude and phase. The discussion of Laguerre-Gauss beams is necessary for introducing students to the orbital angular momentum of the light.

We have successfully introduced this new material to undergraduates in our optics course. As presented in this article, we expanded the treatment of Gaussian beams to include beams in high-order modes, especially the Laguerre-Gauss solutions of the wave equation. This discussion was presented early in course, in a chapter on light waves. Orbital angular momentum was introduced more formally later in the course, after a chapter on polarization. This way we could cover under the unifying theme of momentum, the linear momentum of the light and both forms of angular momentum, spin and orbital. The phase of Gaussian beams was revisited in the chapter on interference. The topic also provided interesting exercises, such as the calculation of interference patterns that could be compared to images of real patterns, like those of Fig. 2. The experiments discussed in this article were used in the laboratory component of the course or in class demonstrations.

Acknowledgments

We thank P.R. Crawford, P.J. Haglin, V. Matos, M.W. Pysher, H.I. Sztul, and R.E. Williams for their contributions to our laboratory experience at Colgate University, and C.H. Holbrow and J. Noe for help and useful discussions.

APPENDIX A: INTERFEROMETER ALIGNMENT

Aligning the Mach Zehnder interferometer requires a systematic approach. Here we describe a method that produces an excellent alignment with not much frustration. This alignment also gets the beam very close to the condition of zero path-length difference. The basis of our alignment is simple: to make all beams travel in directions parallel to the tapped holes of an optical breadboard. We instruct our students to learn this procedure, outlined below, as a basic skill in optics laboratory procedures.

Suppose that we wish to align a beam after it is reflected off a mirror. The alignment goes as follows:

1. The beam is first aimed by eye to be parallel to the holes on the breadboard. We put pairs of screws (with socket or knurled heads) along the same row of holes in two positions: # 1 (near) and # 2 (far). This is shown in "step 1" of Fig. 5.

2. An iris is put in position # 1 with its mount touching the two screws in that position. The iris is then adjusted so that the beam goes through the iris, as shown in "step 2" of Fig. 5.

3. The iris is now put in position # 2, with its mount touching the screws, as in position # 1. If the beam goes through the iris, then it is aligned because from positions # 1 to # 2 the iris has been translated along a line parallel to the holes on the breadboard. If the beam does not go through the iris in position # 2 then the beam must be steered by tilting the mirror until the beam goes through the iris, as shown in "step 3" of Fig. 5.

4. Iterate the previous two steps until the alignment converges.

The interferometer is set up by putting the components one by one. We first put a beam splitter and align it so that the reflected part of the beam is parallel to the rows of holes on

the breadboard, as described above. We follow putting the two mirrors one by one, aligning them so that the steered beams are also parallel to the holes of the breadboard. One of the mirrors is mounted on a translation stage. By this point we must have the two beams intersecting in air. The next step is to put the second beam splitter so that the two beams meet at its beam-splitting surface. We tilt this beam splitter so that the reflected beam is aligned with the holes of the breadboard. Lastly, we adjust the translation stage until the two beams overlap.

---

[1] M.J. Padgett and L. Allen, "Light with a twist in its tail," Contemporary Phys. **41**, 275-285 (2000).

[2] *Natural Focusing and Fine Structure of Light: Caustics and Wave Dislocations*, J.F. Nye (Institute of Physics, Bristol, 1999).

[3] M.V. Berry, "Much Ado About Nothing: Optical Dislocation Lines (Phase Singularities Zeros, Vortices...)," in *Singular Optics*, M.S. Soskin (ed.), *Proc. SPIE* **3487** pp. 1-5, 1998.

[4] *Optics*, E. Hecht (Addison Wesley, Reading, 2002).

[5] *Introduction to Optics* F.L. Pedrotti and L.S. Pedrotti (Prentice Hall, Upper Saddle River, 1993).

[6] A.M. Almeida, E. Nogeira, and M. Belseley, "Paraxial imaging: Gaussian beams versus paraxial-spherical waves," Am. J. Phys. **67**, 428-433 (1999).

[7] *Lasers*, P.W. Milonni and J.H. Eberly (John Wiley & Sons, New York, 1988).

[8] P. Nachman, "Mach-Zehnder interferometer as an instructional tool," Am. J. Phys. **63**, 39-43 (1995).

[9] *Lasers* A.E. Siegman (University Science Books, Mill Valley, 1986).

[10] M.W. Beijersbergen, L. Allen, H.E.L.O. van der Veen, and J.P. Woerdman, "Astigmatic laser mode converters and transfer of orbital angular momentum." Optics. Commun. **96**, 123-132 (1993).

[11] M. Padgett, J. Arlt, and N.Simpson, "An experiment to observe the intensity and phase structure of Laguerre-Gaussian laser modes," Am. J. Phys. **64**, 77-82 (1996).

[12] J. Brandenberger, "Experiments in Laser Physics and Spectroscopy for Undergraduates," (Lawrence University, 2005).

[13] E. Zauderer "Complex argument Hermite-Gaussian and Laguerre-Gaussian beams," J. Opt. Soc. Am. **3**, 465-469 (1986).

[14] M. Brambilla, F. Battipede, L.A. Lugiato, V. Penna, F. Prati, C. Tamm, and C.O. Weiss, "Transverse laser patterns. I. Phase singularity crystals," Phys. Rev. A **43** 5090-5113 (1991).

[15] N.R. Heckenberg, R. McDuff, C.P. Smith, and A.G. White, "Generation of optical phase singularities by computer-generated holograms," Opt. Lett., **17**, 221-223 (1992).

[16] G.F. Brand, "Phase singularities in beams," Am. J. Phys. **67**, 55-60 (1999).

[17] E.J. Galvez, P.R. Crawford, H.I. Sztul, M.J. Pysher, P.J. Haglin, and R.E. Williams, "Geometric phase associated with mode transformation of optical beams bearing orbital angular momentum," Phys. Rev. Lett. **90**, 2039011-4 (2003).

[18] L. Allen, M.W. Beijersbergen, R.J.C. Spreeuw, and J.P. Woerdman, "Orbital angular momentum of light and the transformation of Laguerre-Gaussian laser modes," Phys. Rev. A **45**, 8185-8189 (1992).

[19] J. Durnin, J.J. Miceli, Jr., and J.H. Eberly, "Diffraction-free beams," Phys. Rev. Lett. **58**, 1499-1501 (1987).

[20] J.C. Gutierrez-Vega, M.D. Iturbe-Castillo, and S. Chavez-Cerda, "Alternative formulation for invariant optical fields: Mathieu beams," Opt. Lett. **25**, 1493-1495 (2000).

[21] L. Allen, M.J. Padgett, and Babiker, "The orbital angular momentum of light," Progress in Optics XXXIX (Elsevier Science B.V., 1999).

[22] *Optical Angular Momentum*, L. Allen, S.M. Barnett,and M.J. Padgett (Institute of Physics, Bristol, 2003).

[23] J.E. Curtis and D.E. Grier, "Structure of Optical Vortices," Phys. Rev. Lett. **90**, 133901 (2003).

[24] H. He, M.E.J. Friese, N.R. Heckenberg, and H. Rubinsztein-Dunlop, "Direct observation of transfer of angular momentum to absorptive particles from a laser beam with a phase singularity," Phys. Rev. Lett. **75**, 826-829 (1995).

[25] N.B. Simpson, K. Dholakia, L. Allen, and M.J. Padgett, "Mechanical equivalence of spin and orbital angular momentum of light: an optical spanner," Opt. Lett. **22**, 52-54 (1997).

[26] C. Rotschild, S. Zommer, S. Moed, O. Hershcovitz, and S.G. Lipson, "Adjustable spiral phase plate," Appl. Opt. **43**, 2397-2399 (2004).

FIG. 1: Mach-Zehnder interferometer for studying the phases of optical beams. The basic components are two beam splitters (BS) and two mirrors (M), with one mirror mounted on a translation stage (T). A lens (L) can be added to one of thte arms for observing the pattern produced with the light from the other arm. A computer-generated grating (G) can be inserted in one of the arms to produce high-order modes.

FIG. 2: Pictures of images of interference patterns produced with the Mach-Zehnder interferometer and recorded with a CCD camera. In Patterns (a,b), (c,d) and (e,f) the signal beams were zero-order Gaussian, first-order Hermite-Gauss, and first-order Laguerre-Gauss, respectively. In patterns (a,c,e) the reference beam was unexpanded and non-collinear, and in (b,d,f) the reference beam was expanded and collinear.

FIG. 3: Computer-generated holograms to generate first-order Hermite-Gauss beams (a), and Laguerre-Gauss beams (b). The lower images are photos of the diffraction patterns that result when the gratings above are illuminated by a zero-order beam. The gratings used to produce the patterns in the images did not have the same density of fringes.

FIG. 4: Perspective view of the wave-front of a first-order Laguerre-Gauss beam. The helical surface is formed by points where the wave has the same phase (crests, in the picture).

FIG. 5: Procedure to align a laser beam to the rows of holes on an optical breadboard (see text).

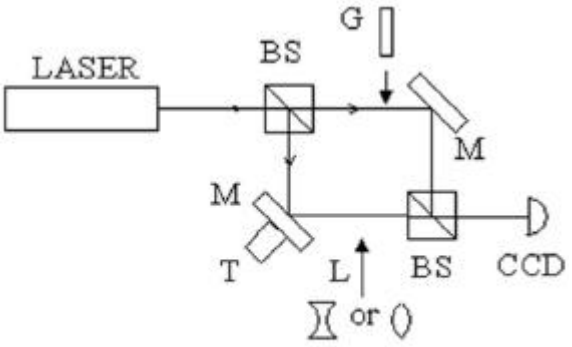

Galvez Fig. 1

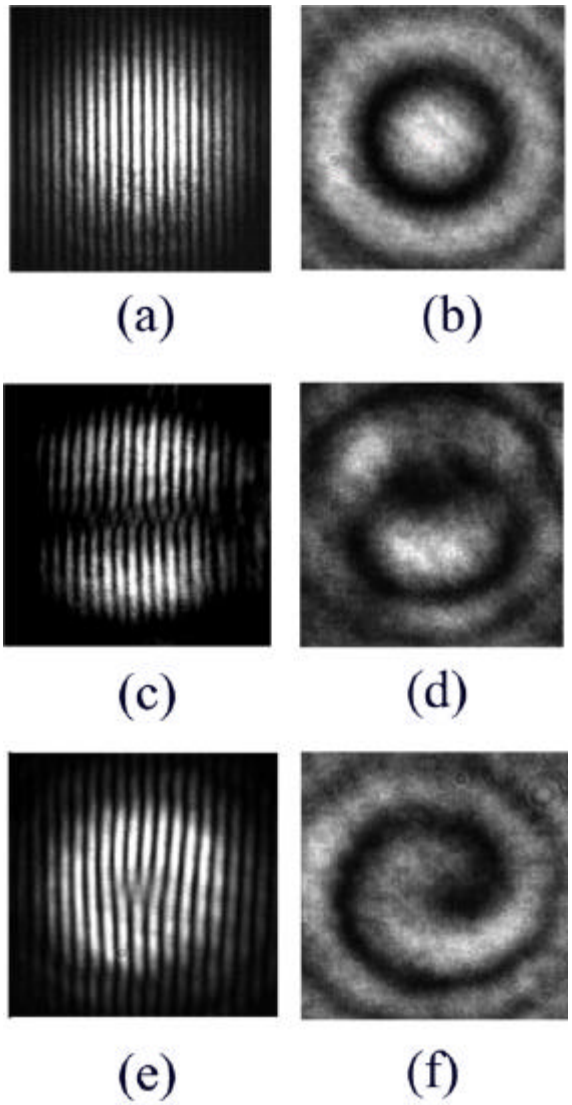

Galvez Fig. 2

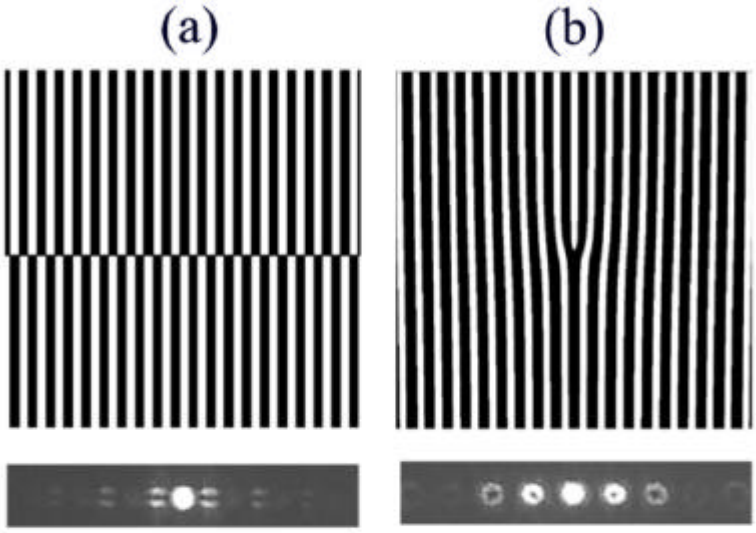

Galvez Fig. 3

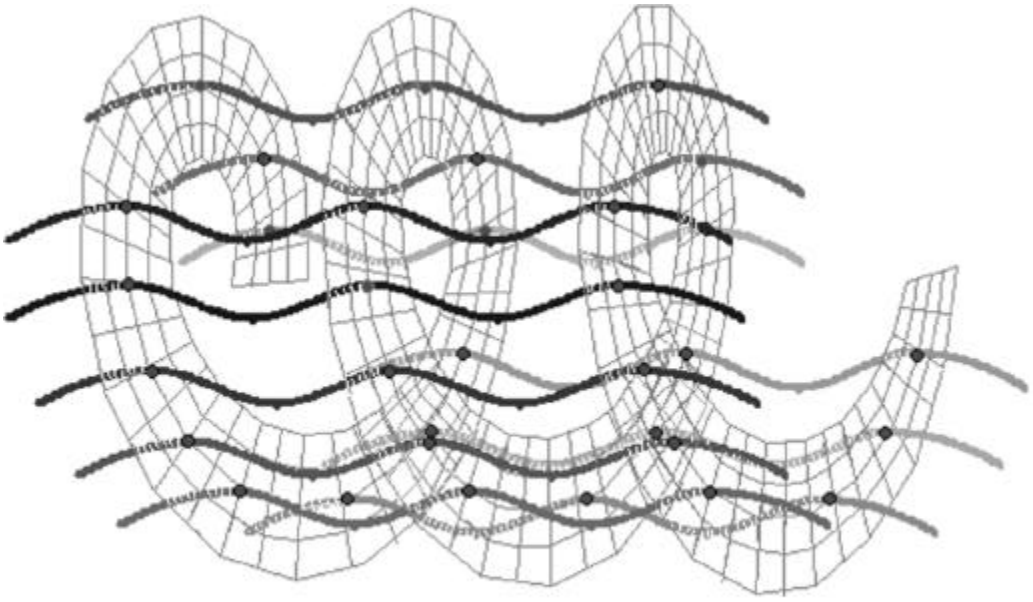

Galvez Fig. 4

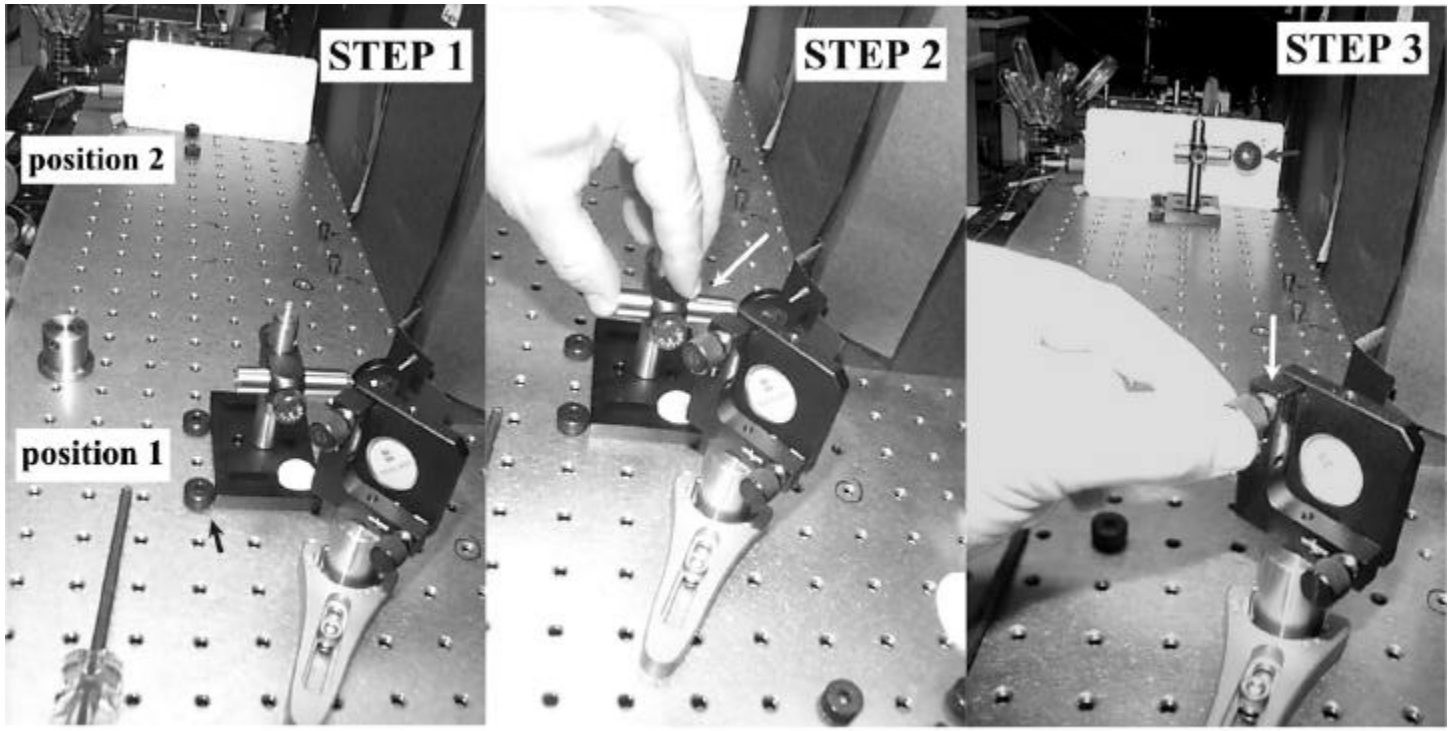

Galvez Fig. 5